



REFRACTIVE INDEX AND PROPAGATION OF LIGHT IN NANOELLIPSOIDAL METAL AND DIELECTRIC COMPOSITE

By
Hailu Tegegn Desta

SUBMITTED IN PARTIAL FULFILLMENT OF THE
REQUIREMENTS FOR THE DEGREE OF
MASTER OF SCIENCE IN PHYSICS

AT
JIMMA UNIVERSITY
JIMMA, ETHIOPIA
NOVEMBER 2015

© Copyright by Hailu Tegegn Desta, 2015
hailutegegndesta@gmail.com

JIMMA UNIVERSITY
DEPARTMENT OF
PHYSICS

The undersigned hereby certify that they have read and recommend to the School of Graduate Studies for acceptance a thesis entitled **“Refractive index and propagation of light in nanoellipsoidal metal and dielectric composite”** by **Hailu Tegegn Desta** in partial fulfillment of the requirements for the degree of **Master of Science in Physics**.

Dated: November 2015

Supervisors:

Reader:

JIMMA UNIVERSITY

Date: **November 2015**

Author: **Hailu Tegegn Desta**

Title: **Refractive index and propagation of light in
nanoellipsoidal metal and dielectric composite**

Department: **Physics**

Degree: **M.Sc.** Convocation: **February** Year: **2016**

Permission is herewith granted to Jimma University to circulate and to have copied for non-commercial purposes, at its discretion, the above title upon the request of individuals or institutions.

Signature of Author

THE AUTHOR RESERVES OTHER PUBLICATION RIGHTS, AND NEITHER THE THESIS NOR EXTENSIVE EXTRACTS FROM IT MAY BE PRINTED OR OTHERWISE REPRODUCED WITHOUT THE AUTHOR'S WRITTEN PERMISSION.

THE AUTHOR ATTESTS THAT PERMISSION HAS BEEN OBTAINED FOR THE USE OF ANY COPYRIGHTED MATERIAL APPEARING IN THIS THESIS (OTHER THAN BRIEF EXCERPTS REQUIRING ONLY PROPER ACKNOWLEDGEMENT IN SCHOLARLY WRITING) AND THAT ALL SUCH USE IS CLEARLY ACKNOWLEDGED.

Table of Contents

Table of Contents	vi
List of Figures	vii
Abstract	ix
Acknowledgements	x
1 Introduction	1
1.1 Background of the study	1
1.2 Statement of the Problem	3
1.3 Objectives	3
1.3.1 General Objective	3
1.3.2 Specific Objectives	3
1.4 Significance of the Study	4
2 Theoretical Background	5
2.1 Maxwell equations	5
2.2 Nonlinear optics	6
2.3 Lorentz local field and oscillator models	8
2.3.1 Lorentz local field	8
2.3.2 Lorentz model	9
2.3.3 Drude model	9
2.4 The Maxwell-Garnett effective medium theory	9
2.5 Refractive index and group velocity	10
2.5.1 Refractive index	10
2.5.2 Phase and group velocity	11
3 Methods and Materials	13
3.1 Methods	13
3.2 Soft wares	13

4	Results and Discussion	14
4.1	Analytical description of refractive index and group velocity in composite with pure metal ellipsoidal nanoparticles	14
4.1.1	When all pure metal inclusions are aligned in passive dielectric material	16
4.1.2	Effective dielectric function of the composite	18
4.1.3	When pure metal ellipsoidal nanoparticles are randomly oriented in passive dielectric material	19
4.1.4	Refractive index in composite with pure metal ellipsoidal nanoparticles	22
4.1.5	Group velocity of light pulses in the composite with with pure metal ellipsoidal nanoparticles	22
4.2	Analytical description of refractive index and group velocity in composite with metal shell-dielectric core ellipsoidal nanoparticles	23
4.2.1	When all metal shell-dielectric core ellipsoidal nanoparticles are aligned in passive dielectric material	24
4.2.2	When the metal shell-dielectric core ellipsoidal nanoparticles are randomly oriented in passive dielectric material	27
4.2.3	Effective dielectric function of the composite medium	28
4.2.4	Refractive index of the composite medium	29
4.2.5	Group velocity in the composite with ellipsoidal metal shell-dielectric core nanoparticles	29
4.3	Numerical description of refractive index in composite with ellipsoidal pure metal nanoparticles	30
4.3.1	The effect of geometrical factor of the ellipsoidal pure metal nanoparticles on the refractive index	30
4.3.2	Effect of the concentration of the ellipsoidal metallic nanoparticles in the composite on the refractive index	31
4.4	Numerical description of refractive index in composite with ellipsoidal metal shell-dielectric core nanoparticles	33
4.4.1	The effect of geometrical factor of the ellipsoidal metal shell-dielectric core nanoparticles on the refractive index	33
4.4.2	The effect of the concentration of the ellipsoidal metal shell-dielectric core nanoparticles on the refractive index	34
4.4.3	The effect of the metal volume fraction in the metal shell-dielectric core nanoparticles on the refractive index	36
4.5	Numerical description of group velocity in composite with ellipsoidal pure nanoparticles	37
4.5.1	The effect of the geometrical factor of the ellipsoidal pure metal nanoparticles on group velocity	38
4.5.2	The effect of concentration of ellipsoidal pure metal nanoparticles on the group velocity	39

4.6	Numerical description of group velocity in composite with metal shell-dielectric core ellipsoidal nanoparticles	41
4.6.1	The effect of the geometrical factor of the metal shell-dielectric core ellipsoidal nanoparticles on the group velocity in composite	41
4.6.2	The effect of concentration of metal shell-dielectric core ellipsoidal nanoparticles on the group velocity	42
4.6.3	The effect of metal volume fraction in the metal shell-dielectric core ellipsoidal nanoparticles on group velocity	44
5	Conclusion and future outlook	46
	Bibliography	50

List of Figures

4.1	Ellipsoidal pure metallic nanoparticle	15
4.2	metal shell-dielectric core nanoellipsoid	23
4.3	The real part of the refractive index n_r versus frequency z of applied field for three values of geometrical factor in composite with pure metal nanoellipsoidal inclusions	31
4.4	The real part of refractive index n_r versus frequency of applied field z for three values volume filling factor of the pure metal nanoellipsoidal inclusions	32
4.5	The real part of refractive index n_r versus applied field frequency z for three values of geometrical factor in composite with metal shell-dielectric core nanoellipsoids	34
4.6	The real part of refractive index n_r versus applied field frequency z for three values of concentration of metal shell-dielectric core nanoellipsoids	35
4.7	The real part of refractive index n_r versus applied field frequency z for three values of the metal volume fraction in the metal shell-dielectric core nanoellipsoids	37
4.8	Group velocity normalized to speed of light in free space $\frac{v}{c}$ versus applied field frequency z in composite with pure metal nanoellipsoids for three geometrical factor values	39
4.9	Group velocity to speed of light in free space $\frac{v}{c}$ versus applied field frequency z in composite with pure metal nanoellipsods for three values of their concentration	40
4.10	Group velocity to speed of light in free space $\frac{v}{c}$ versus applied field frequency z in composite with metal shell-dielectric core nanoellipsoids for three geometrical factor values	42

4.11	Group velocity to speed of light in free space $\frac{v}{c}$ versus applied field frequency z in composite with metal-shell dielectric core nanoellipsoids for three values of their concentration	43
4.12	Group velocity to speed of light in free space $\frac{v}{c}$ versus applied field frequency z in composite with metal-shell dielectric core nanoellipsoids for three values of the metal volume fraction in the ellipsoids	45

Abstract

Refractive index and propagation of electromagnetic pulses are studied analytically and numerically in a medium with nanoellipsoidal metal/dielectric composites. The cases when all nanoellipsoidal inclusions are aligned to the direction of the incident field and when they are randomly distributed are considered for pure metal type and confocal metallic shell and dielectric core type inclusions embedded in a passive host medium. Based on long wave approximation and the effective dielectric response of the medium the effects of geometrical factor, filling factor and orientation of the inclusions on the refractive index and group velocity are described analytically and computationally.

Key words; Polarization, Dielectric function, Refractive index, Anomalous dispersion

Acknowledgements

First, I would like to thank the Almighty GOD. It is only due to His blessings that I have been able to accomplish this work.

Next, I would like to express my gratitude, appreciation and respect to my advisor, Dr Sisay Shewamare, for his guidance, invaluable advice and kindness throughout this study. I would like to express my heartfelt appreciation and respect to my co-advisor, Mr Getnet Melese, for his unreserved support while carrying out this research work. I would like to thank my instructors and all staff members in the department of physics and my friends for their supports during my study. Without their help this work would not have been possible. Finally I would like to express my thank to my wife for her support throughout this work.

Refractive index and propagation of light in nanoellipsoidal metal and dielectric composite

Hailu Tegegn Desta

November 10, 2015

Chapter 1

Introduction

1.1 Background of the study

The optical property of small metallic particles has been studied long ago [1,2]. However, nonstructural metallic materials become the focus of intense research in recent years. This revival of interest is due to the recent advances that allow metals to be structured and characterized on the nanometer scale with well defined sizes and shapes [2–4] as well as many possible applications have been realized to use these materials in different fields such as optoelectronics, biological and medical sciences. Now in these days nanometallic materials are novel parts in many devices like, for optical communications [5], to energy harvesting [6] and optical bio sensors with enhanced sensitivity [7,8].

Metallic nanoparticles have exceptional optical properties that are not observed in the bulk material phase [9–12]. This optical effect is caused by strong interaction between light and the conduction electrons that are confined in the small volume of the particle. Under the influence of oscillating electromagnetic field the negatively charged conduction electrons perform a collective oscillation with respect to the positive ion background creating an effective charge at the surface that results in a restoring force, the collective excitation of the electrons at the interface is called a localized surface plasmon [8,13]. The localized surface plasmons are due to the small scale size of the metal unlike the ordinary surface plasmon of the extended metal surfaces. In a nanostructured metal the

localized surface plasmon cause strongly enhanced optical absorption and scattering cross sections, because they readily couple to optical far fields and also light can be confined to and manipulated on a scale smaller than the wavelength of the light, only a few hundred nanometers [14, 15]. An example to this phenomenon is the high transmission efficiency of light through sub wavelength holes in a metal screen [16, 17].

The resonance wavelength of the localized surface plasmon to a nanoparticle is uniquely determined by its shape, size and the nature of host material embedding it. Therefore, the nanoparticle plasmon frequency can be tuned to a frequency range depending on the required applications [2, 4, 17–19]. For example in optical coherent tomography or therapeutic agents for biomedical applications it is advantageous to tune the particle resonant frequency to the near infrared region between 650nm and 900nm and this tunability is provided by properly designing the shape, size, orientation, concentration and composition of nanometallic inclusions in the host medium [18].

The refractive index of a material is the key parameter that affects all optical properties. Any modification of the refractive index, by any means, leads to new optical properties of absorption, dispersion and transmission of the medium [20]. Therefore a study about refractive index of material media is vary essential to know about the optical properties the material. In this paper, we have shown that how refractive index and propagation of light pulses are affected by the geometrical factor, orientation, composition, and the concentration of nanoellipsoidal pure metal and metal covered dielectric core particles embedded in aligned manner and randomly in a passive host materials.

We have already mentioned some motivational background concepts at the beginning of the introduction, in this part we also included the statements of the problem, the objectives and significance of the work. The rest of this thesis is organized as follows;

In chapter 2 we present a short review of basic theoretical concepts about electromagnetism and optical response of materials.

In chapter 3 we explain the analytical and numerical methods employed in this work.

In chapter 4 we show derivation of some model equations. Using these equations we give theoretical analysis about resonance conditions, polarizabilities, effective dielectric functions and refractive index. Then we show numerical descriptions of the results with figures which illustrate the variation of refractive index and group velocity with the frequency of incident field for the different cases.

Finally in chapter 5 we discuss the results and draw some conclusions.

1.2 Statement of the Problem

In this study we tried to address the following major issues for a nanoellipsoidal metal/dielectric composite medium when the identical inclusions are pure metals and when they are identical metal shell-dielectric core composite:

- How the geometrical factor, concentration and orientation of the inclusions and fraction of the metal part in the inclusions affect the refractive index and propagation of light pulses in the medium.
- How the variations of refractive index and group velocity with geometrical factor, concentration and orientation of pure metal inclusions differ from their corresponding variations for the case of metal shell dielectric core inclusions.

1.3 Objectives

1.3.1 General Objective

- To study analytically and numerically about the refractive index and propagation of light pulses in nanoellipsoidal metal and dielectric composite material.

1.3.2 Specific Objectives

The the specific objectives are:

- To calculate the refractive index and group velocity for the different values of geometrical factors and concentrations of identical ellipsoidal metallic nanoparticles embedded in passive dielectric material for the cases when the ellipsoids are aligned and randomly oriented.
- To calculate the refractive index and group velocity for the different values of geometrical factors, concentrations and metal fractions of identical ellipsoidal metal shell-dielectric core nanoparticles embedded in passive dielectric material for the cases when the ellipsoids are aligned and randomly oriented.
- To describe propagation of light in each of the above cases using the computed group velocities.
- To compare and contrast results computed to composites with aligned ellipsoids to that with randomly oriented ellipsoids.

1.4 Significance of the Study

Currently the optical response of metallic nanoparticles is a topic of great interest which is investigated both theoretically and experimentally for the purposes of further understanding of the optical effects and to exploit these novel effects in broad activities of applications. So this study will contribute important informations to researchers and experts in the areas of nanoparticles and their applications.

Chapter 2

Theoretical Background

2.1 Maxwell equations

Jams C. Maxwell modified and restated the basic laws in electromagnetism in four equations which are known as Maxwell equations for the propagation of electromagnetic waves in matter, in differential form they can expressed as [21, 22]:

$$\nabla \cdot \mathbf{D} = \rho, \quad (2.1.1)$$

$$\nabla \times \mathbf{E} = -\frac{\partial \mathbf{B}}{\partial t}, \quad (2.1.2)$$

$$\nabla \cdot \mathbf{B} = 0, \quad (2.1.3)$$

$$\nabla \times \mathbf{H} = \mathbf{J} + \frac{\partial \mathbf{D}}{\partial t}, \quad (2.1.4)$$

where \mathbf{E} is electric field, \mathbf{D} is electric displacement, \mathbf{H} is magnetic field intensity, \mathbf{B} is magnetic induction, ρ is the electric charge density, and \mathbf{J} is the electric current density, which is related to the electric field by:

$$\mathbf{J} = \sigma \mathbf{E}, \quad (2.1.5)$$

where σ is conductivity of the medium.

From equations (2.1.1) and (2.1.4) we can derive the equation of continuity

$$\nabla \cdot \mathbf{J} + \rho \frac{\partial \rho}{\partial t} = 0. \quad (2.1.6)$$

From the Maxwell equations we can obtain equation for the force \mathbf{F} on a charge exposed to an electromagnetic field as [22]:

$$\mathbf{F} = \rho\mathbf{E} + \frac{\mathbf{J} \times \mathbf{B}}{c} \quad (2.1.7)$$

where c is the speed of light in free space.

Electromagnetic waves applied on a material induce polarization and magnetization. Polarization \mathbf{P} is the density of electric dipole moments and magnetization \mathbf{M} is the density of magnetic moments in the material and their relation to their corresponding fields are given by:

$$\mathbf{D} = \varepsilon_o\mathbf{E} + \mathbf{P}, \quad (2.1.8)$$

$$\mathbf{H} = \frac{\mathbf{B}}{\mu_o} - \mathbf{M}, \quad (2.1.9)$$

where ε_o and μ_o are respectively electric permittivity and magnetic permeability for free space. For high frequency electromagnetic waves which are referred as optical waves the magnetization of many materials especially metals and dielectrics is very weak compared to their polarization for this reason the optical response of materials mostly described by the polarization. Using the Maxwell equations (2.1.2) and (2.1.4) with equation (2.1.6) we can derive equation for electromagnetic wave in material medium and written as [23]:

$$\nabla \times \nabla \times \mathbf{E} + \frac{1}{c^2}\partial^2\mathbf{E}/\partial t^2 + \frac{\sigma}{\varepsilon_o c^2}\partial\mathbf{E}/\partial t + \frac{1}{\varepsilon_o c^2}\partial^2\mathbf{P}/\partial t^2 = 0. \quad (2.1.10)$$

2.2 Nonlinear optics

In most optical phenomena the response of the material to electromagnetic radiation is studied in terms of the relation between the induced polarization and the applied electric field. Linear optics considers the linear dependence of the polarization on the electric field that is expressed as [23]:

$$\mathbf{P}(t) = \varepsilon_o\chi^{(1)}\mathbf{E}(t), \quad (2.2.1)$$

where $\mathbf{P}(t)$ and $\mathbf{E}(t)$ are respectively the time varying polarization and electric field and $\chi^{(1)}$ is the linear susceptibility of the medium. Nonlinear optics deals about optical phenomena considering the nonlinear relations between the polarization and the electric field and equation (2.1.11) is generalized by the expression of $\mathbf{P}(t)$ as a power series expansion of $\mathbf{E}(t)$ [23]:

$$\mathbf{P}(t) = \varepsilon_o[\chi^{(1)}\mathbf{E}(t) + \chi^{(2)}\mathbf{E}^2(t) + \chi^{(3)}\mathbf{E}^3(t) + \dots], \quad (2.2.2)$$

where $\chi^{(2)}$ and $\chi^{(3)}$ are respectively are the second-order and third order susceptibilities. As seen in equation (2.2.2) the polarization is combination of both linear and nonlinear parts and can be written as:

$$\mathbf{P}(t) = \mathbf{P}^{(1)}(t) + \mathbf{P}^{NL}(t). \quad (2.2.3)$$

From equations (2.1.8) and (2.2.3) we obtain relation between the nonlinear polarization \mathbf{P}^{NL} and the electric field \mathbf{E} and electric displacement \mathbf{D}

$$\mathbf{D}(t) = \varepsilon_o(1 + \chi^{(1)})\mathbf{E}(t) + \mathbf{P}^{NL}(t). \quad (2.2.4)$$

Combining equations (2.2.1) and (2.2.3) with (2.1.10) we obtain the equation of electromagnetic waves with a nonlinear term [23]:

$$\nabla \times \nabla \times \mathbf{E} + \frac{\sigma}{\varepsilon_o c^2} \partial \mathbf{E} / \partial t + \frac{1 + \chi^{(1)}}{c^2} \partial^2 \mathbf{E} / \partial t^2 + \frac{1}{\varepsilon_o c^2} \partial^2 \mathbf{P}^{NL} / \partial t^2 = 0. \quad (2.2.5)$$

This equation shows that the nonlinear response of the medium acts as a source term and it become significant only for high intensity radiations, which are lasers, for low intensity radiations the nonlinear term vanishes and become equation to the case of linear response [23]:

$$\nabla \times \nabla \times \mathbf{E} + \frac{\sigma}{\varepsilon_o c^2} \frac{\partial \mathbf{E}}{\partial t} + \frac{(1 + \chi^{(1)})}{c^2} \frac{\partial^2 \mathbf{E}}{\partial t^2} = 0 \quad (2.2.6)$$

2.3 Lorentz local field and oscillator models

2.3.1 Lorentz local field

The linear susceptibility is defined in terms of the macroscopic electric field \mathbf{E} and polarization \mathbf{P} of the medium as in equation (2.2.1) but the polarizability α of nanoparticles has to be defined in microscopic form in terms of local or effective electric field \mathbf{E}_{loc} at the site of the particle and its dipole moment \mathbf{p}

$$\mathbf{P} = N\mathbf{p}, \quad (2.3.1)$$

$$\mathbf{p} = \alpha\mathbf{E}_{loc}. \quad (2.3.2)$$

Based on the assumption of a spherical cavity with the molecule located at the center Lorentz obtained a relation between microscopic local field with the macroscopic field as [10]:

$$\mathbf{E}_{loc} = \mathbf{E} + \frac{\mathbf{P}}{3\epsilon_0} \quad (2.3.3)$$

The expression of linear susceptibility in terms of polarizability is obtained from equations (2.2.1), (2.3.2) and (2.3.3) and it is expressed as:

$$\chi^{(1)} = \frac{N\alpha}{1 - \frac{N\alpha}{3}}, \quad (2.3.4)$$

where N is the number of particles per unit volume. Equation (2.3.4) is known as Lorentz-Lorentz relation. Then the equation for dielectric function in terms of polarizability is written as:

$$\frac{\epsilon^{(1)} - \epsilon_h}{\epsilon^{(1)} + 2\epsilon_h} = \frac{N\alpha}{3}. \quad (2.3.5)$$

Equation (2.3.5) is known as Clausius Mossotti relation, where $\epsilon^{(1)}$ is dielectric function of small spherical particle and ϵ_h is the dielectric function of the embedding host material [23].

2.3.2 Lorentz model

Lorentz model is a theory in which electrons and ions in materials were treated as harmonic oscillators which are under the influence of deriving local electric field and certain damping force. Based on this consideration the expression for dielectric function of the particle can be obtained as [10]:

$$\epsilon^{(1)} = 1 + \chi^{(1)} = \epsilon_{\infty} + \frac{\omega_p^2}{\omega_o^2 - \omega^2 - i\gamma\omega}, \quad (2.3.6)$$

where ω is the frequency of the applied field, ω_o is resonance frequency of the oscillator and ω_p is the plasma frequency that is given by the relation

$$\omega_p = \sqrt{\frac{Ne^2}{m\epsilon_o}}, \quad (2.3.7)$$

where m is electron effective mass, γ is the damping parameter and ϵ_{∞} is dielectric function when oscillation is at much higher frequencies.

2.3.3 Drude model

This is a theory which modifies the Lorentz model to free electrons by letting zero the value of the force constant to the Lorentz oscillator so $\omega_o = 0$ in equation (2.3.6) gives the Drude dielectric function for free electron [23].

$$\epsilon^{(1)} = \epsilon_{\infty} - \frac{\omega_p^2}{\omega^2 + i\gamma\omega}. \quad (2.3.8)$$

2.4 The Maxwell-Garnett effective medium theory

Effective medium theories are models which describe composite heterogeneous materials through effective material properties determined based on certain approximations and applying statistical averaging method to the microscopic Maxwell equations. Maxwell-Garnett effective medium approximation is the easiest and widely used model for calculating effective dielectric quantities of composite materials consisting many components [24–29] and in this model the embedding or background material is considered as host

medium or matrix and the embedded components are considered as inclusions.

The Maxwell-Garnett approximation is applicable to linear medium with inclusions whose size is very small compared to the wavelength of light waves in the effective medium so that the electric field in the inclusions is assumed to be uniform and the inclusions are separated by large distances in other words their concentration is very dilute so the particles are assumed to be noninteracting. For a medium composed of a single type or identical ellipsoidal inclusions embedded randomly in a host material Maxwell-Garnett formula for the effective dielectric function is given by [10]:

$$\epsilon_{eff} = \frac{(1-f)\epsilon_h + f\beta\epsilon}{1-f+f\beta}, \quad (2.4.1)$$

$$\beta = \frac{1}{3} \sum \lambda_k, \quad (2.4.2)$$

$$\lambda_k = \frac{\epsilon_h}{\epsilon_h + L_k(\epsilon - \epsilon_h)}, \quad (2.4.3)$$

where $k = 1, 2, 3$ represent the three principal axis of the ellipsoidal inclusions, L_k is geometrical factor of the ellipsoids to the k^{th} principal axes of the ellipsoids, ϵ and ϵ_h are respectively the dielectric functions of the inclusions and the host material.

2.5 Refractive index and group velocity

2.5.1 Refractive index

Refractive index and dielectric function are often used to describe optical properties of materials. They are generally complex quantities which can be affected by frequency and intensity or amplitude of the incident light waves. For a nonmagnetic, isotropic and linear medium they are related by:

$$n = \sqrt{\epsilon} \quad (2.5.1)$$

where the complex refractive index $n = n_r + \iota n_i$ and the complex dielectric function of the material $\epsilon = \epsilon_r + \iota \epsilon_i$. Then the real and imaginary parts are related by [10, 21, 22]:

$$n_r = \sqrt{\frac{1}{2}(\epsilon_r + \sqrt{\epsilon_r^2 + \epsilon_i^2})} \quad (2.5.2)$$

$$n_i = \sqrt{\frac{1}{2}(-\epsilon_r + \sqrt{\epsilon_r^2 + \epsilon_i^2})} \quad (2.5.3)$$

2.5.2 Phase and group velocity

Light from a poly monochromatic source is composition of different electromagnetic waves with different frequencies. The frequency ω and wave number k depend on each other as given by:

$$\omega = \frac{ck}{n_r}. \quad (2.5.4)$$

Phase velocity is the rate at which the phase of the wave propagate in space, that is, the velocity at which the phase of any one frequency component of the wave will propagate and it is expressed as [10, 22]:

$$v_p = \frac{\omega}{k}. \quad (2.5.5)$$

Group velocity is the rate at which the change in amplitude of the wave envelop or packet will propagate. If the intensity of a signal varies with time, i.e., the spectrum of the signal has finite width, the group velocity stands for the propagation speed of the intensity modulation [30] and it is expressed by the relation

$$v_g = \frac{d\omega}{dk}, \quad (2.5.6)$$

$$v_g = \frac{c}{n_g}, \quad (2.5.7)$$

$$n_g = n_r + \omega \frac{dn_r}{d\omega}, \quad (2.5.8)$$

where c is speed of light in free space and n_g is known as group index.

The frequency interval in which $\frac{dn_r}{d\omega} > 0$ is referred as normal dispersion region and $v_g < c$.

The frequency interval in which $\frac{dn_r}{d\omega} < 0$ is called region of anomalous dispersion and some times in the anomalous region apparently $v_g > c$. Such virtual light whose speed exceed the speed of light in free space is known as superluminal light.

The frequency distribution with respect to the wave vector k is expressed according to the series expansion at $k = k_o$ at which the the frequency is central maximum, ω_o ,

$$\omega(k) = \omega_o + \frac{d\omega}{dk}(k - k_o) + \dots \quad (2.5.9)$$

In the equation (2.5.9) group velocity appear in the second term. Therefore this equation has meaning in the case of weak dispersion of $\omega(k)$ for strong dispersions the higher terms in this equation must be taken in to account and in this case group velocity loses its physical meaning [30].

Chapter 3

Methods and Materials

3.1 Methods

To investigate and to solve the stated problems we employed analytical method that is derivation of equations based on the theoretical concepts. and we applied the equations for the numerical computations of the refractive index and group velocity. The variation of refractive index and group velocity with the different values of the parameters of the nanoellipsoidal inclusions analyzed numerically with the help of computational tools;using soft wares.

3.2 Soft wares

The soft wares used in this project are:

Matlab to develop and process soft ware codes for the numerical simulation of the equations. And plotting figures which show the results.

Mathematica is used as alternative soft ware for managing long analytical and numerical expressions. Because it is preferable in simplifying and handling bulged equations.

Latex to process the edition and compilation of the thesis paper with the standard quality.

Chapter 4

Results and Discussion

4.1 Analytical description of refractive index and group velocity in composite with pure metal ellipsoidal nanoparticles

The refractive index of a medium is calculated from the dielectric function that is determined from the polarizability of the inclusions. So we need expression for the polarizability of the nanoellipsoidal metallic particle and this can be derived from the electric potential distribution in and out side the ellipsoidal particle.

The dilute concentration of particles lead us to neglect dipole-dipole interactions between the particles and long wave approximation help us to assume uniform electric field in the particles. Consider an ellipsoidal metallic particle with semi axis, a , b and c , where $a > b > c$. Assume the particle is embedded in passive host material and an incident field E_o is applied parallel to a principal axis, for the instance consider that the semi major axis c is parallel to the field, as shown in the following figure. The potential distribution can be described using ellipsoidal coordinates (ξ, η, ζ) and the potential function ϕ satisfies the Laplace equation. The relations between the cartesian (x, y, z) and the ellipsoidal coordinates can be used to express the Laplace equation in terms of ellipsoidal coordinates. The solutions to this equation are the ellipsoidal harmonic potentials at the different confocal ellipsoidal surfaces described by ξ . These harmonic potentials are multiples of the potential ϕ_o due to the applied field E_o and they can be written as [10]:

$$\phi_o = -E_o Z$$

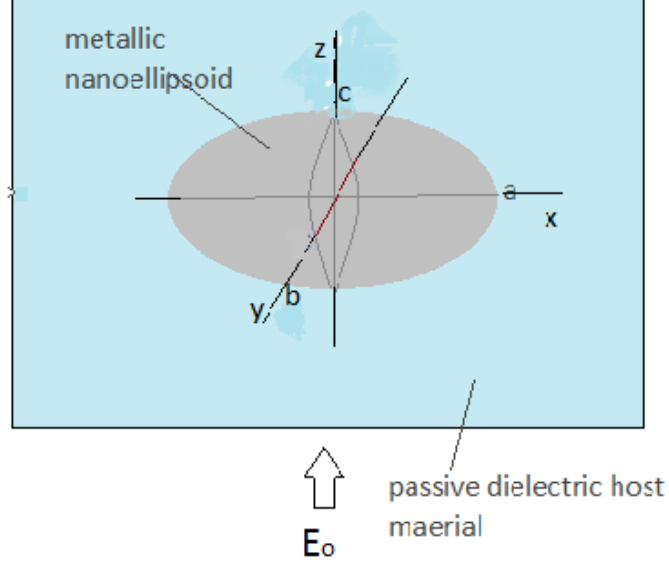


Figure 4.1: Ellipsoidal pure metallic nanoparticle embedded in passive dielectric host material

$$\phi_m = A\phi_o \quad (4.1.1)$$

$$\phi_p = BI\phi_o \quad (4.1.2)$$

$$\phi_h = (1 - BI)\phi_o \quad (4.1.3)$$

$$I = \int_{\xi}^{\infty} \frac{dq}{(q + c^2)f(q)} \quad \text{and} \quad f(q) = [(q + a^2)(q + b^2)(q + c^2)]^{1/2} \quad (4.1.4)$$

where ϕ_p , ϕ_m , and ϕ_h are respectively the potentials due to the polarized particle, inside the metallic particle and outside the particle in the host material. A and B are constants, I is an integral factor, for the points on the ellipsoidal metal surface $\xi = 0$ in this case $I = \frac{2L}{abc}$, L is the geometrical factor with respect to c , and q is ellipsoidal coordinate.

Applying the boundary conditions for the potentials and normal component of the electric displacement at the metal surface the constants can be determined, and using the equation

(2.3.2) the equation to the polarizability α of the particle is obtained as [10, 31, 32]:

$$\alpha = v \frac{\epsilon_m - \epsilon_h}{\epsilon_h + L(\epsilon_m - \epsilon_h)} \quad (4.1.5)$$

where ϵ_m and ϵ_h are respectively the dielectric functions of the metallic ellipsoidal nanoparticle and the dielectric host material and v is volume of the particle.

4.1.1 When all pure metal inclusions are aligned in passive dielectric material

For identical nanoellipsoidal pure metallic inclusions which are aligned so that their respective principal axis are parallel to each other and when the applied field is parallel to one of their principal axis the polarizability of the particles with respect to this principal axis is given by the relation (4.1.5).

For the passive host material its dielectric function ϵ_h is considered to be a positive real value. For the metallic nanoparticles their dielectric function ϵ_m is taken in Drude form. Then the real and imaginary parts respectively denoted by ϵ_{mr} and ϵ_{mi} can be expressed by:

$$\epsilon_{mr} = \epsilon_\infty - \frac{1}{z^2 + \gamma^2}, \quad (4.1.6)$$

$$\epsilon_{mi} = \frac{\gamma}{z(z^2 + \gamma^2)} \quad (4.1.7)$$

$$z = \frac{\omega}{\omega_p} \quad (4.1.8)$$

$$\gamma = \frac{\tau}{\omega_p} \quad (4.1.9)$$

where z is frequency of the applied field ω to the unit of the plasma frequency ω_p and γ is damping constant that is the frequency of electrons collision τ to the unit of the plasma frequency. With the help of equations (4.1.5) - (4.1.7) and passive host material consideration the real and imaginary parts of the polarizability can be expressed as:

$$\alpha_r = \frac{1}{L} \left(1 - \frac{s_r \epsilon_h}{|s|^2} \right) \quad (4.1.10)$$

$$\alpha_i = \frac{s_i \epsilon_h}{L |s|^2} \quad (4.1.11)$$

$$s = L\epsilon_m + (1 - L)\epsilon_h \quad (4.1.12)$$

$$s_r = \epsilon_h + L(\epsilon_{mr} - \epsilon_h) \quad (4.1.13)$$

$$s_i = L\epsilon_{mi}. \quad (4.1.14)$$

It is seen from the equations (4.1.10) and (4.1.11) that both real and imaginary parts decrease with increase in geometrical factor. The resonance conditions are determined from the minimum of the denominators of these equations. Since the imaginary part of s is much smaller than its real part the resonance condition is obtained from $s_r = 0$ and this leads to single resonant point where the real part of the dielectric function for the metallic particles be:

$$\epsilon_{mr} = \left(1 - \frac{1}{L}\right)\epsilon_h \quad (4.1.15)$$

The resonance frequency is obtained from equations (4.1.6) and (4.1.10) as:

$$z_R = \frac{1}{\sqrt{\epsilon_\infty + \left(\frac{1}{L} - 1\right)\epsilon_h}} \quad (4.1.16)$$

From equation (4.1.14) we can reveal that resonance frequency increases when geometrical factor is increased. The values of the real and imaginary polarizabilities at the resonant frequency for weak damping case approximated to be:

$$\alpha_r(z_R) \approx \frac{1}{L} \quad (4.1.17)$$

$$\alpha_i(z_R) \approx \frac{\epsilon_h Z_R^3}{L^2 \gamma} \quad (4.1.18)$$

both polarizability parts decrease when the geometrical factor of inclusions increased and vice versa.

4.1.2 Effective dielectric function of the composite

For the identical and aligned ellipsoidal pure metal nanoinclusions embedded in the passive material with dilute concentration the effective dielectric function of the composite in terms of polarizability of the inclusions is derived from the Maxwell-Garnett effective dielectric formula with equations (2.4.1)-(2.4.3) and (4.1.5) and it can be expressed as:

$$\frac{\epsilon - \epsilon_h}{\epsilon_h + L(\epsilon - \epsilon_h)} = f\alpha \quad (4.1.19)$$

Where $f = NV$ is volume fraction, filling factor or concentration of inclusions in the composite. V is volume of each ellipsoidal particle N is number of particles to the volume of the composite and ϵ is effective dielectric function of the composite medium. For a very dilute concentration of inclusions terms with f^2 are negligible thus neglected from equation (4.1.17) then the real and imaginary parts of the effective dielectric function can be expressed as:

$$\epsilon_r = \left(1 + \frac{f\alpha_r}{1 - 2fL\alpha_r}\right)\epsilon_h \quad (4.1.20)$$

$$\epsilon_i = \frac{f\alpha_i\epsilon_h}{1 - 2fL\alpha_r} \quad (4.1.21)$$

From equations (4.1.18) and (4.1.19) we observe that both parts of the effective dielectric functions will increase with the concentration of the inclusions and decrease as their geometrical factor is increased. Assuming weakly damping case their approximate values at the resonance frequency are:

$$\epsilon_r(z_R) \approx \left(1 + \frac{f}{L}\right)\epsilon_h \quad (4.1.22)$$

$$\epsilon_i(z_R) \approx \frac{f\epsilon_h^2}{L^2\epsilon_{mi}} \quad (4.1.23)$$

4.1.3 When pure metal ellipsoidal nanoparticles are randomly oriented in passive dielectric material

The identical metallic nanoinclusions have the same dielectric function expressed in Drude form. The polarizability of a nanoellipsoidal metallic particle to the direction parallel to a principal axes denoted by $k = 1, 2, 3$ is written as [10, 18]:

$$\alpha_k = v \frac{\epsilon_m - \epsilon_h}{s_k} \quad (4.1.24)$$

$$s_k = \epsilon_h + L_k(\epsilon_m - \epsilon_h) \quad (4.1.25)$$

where α_k is the polarizability of the particle, L_k is the geometrical factor of the particle with respect to the k^{th} principal axes and v is volume of a particle. The real and imaginary parts of polarizability per particle volume are given by:

$$\alpha_{kr} = \frac{1}{L_k} \left(1 - \frac{s_{kr}\epsilon_h}{|s_k|^2} \right) \quad (4.1.26)$$

$$\alpha_{ki} = \frac{s_{ki}\epsilon_h}{L_k |s_k|^2} \quad (4.1.27)$$

$$s_{kr} = \epsilon_h + L_k(\epsilon_{mr} - \epsilon_h) \quad (4.1.28)$$

$$s_{ki} = L_k \epsilon_{mi} \quad (4.1.29)$$

where α_{kr} and α_{ki} are respectively the real and imaginary parts of polarizabilities per particle volume.

Equations (4.1.26) and (4.1.27) show that for a general type of ellipsoid ($a \neq b \neq c$) there is one resonance point with respect to each principal axes and totally there are three possible resonance frequencies [10, 18].

In the composite medium every ellipsoidal particle is polarized to the direction of the applied electric field that may not be parallel to a principal axes but its average polarization is the sum of the average values of its components along the three principal axes. All the three directions of the principal axes are equally probable thus the average polarizability of a randomly oriented ellipsoidal particle is expressed by [10]:

$$\alpha_{av} = \frac{1}{3}(\alpha_1 + \alpha_2 + \alpha_3) \quad (4.1.30)$$

$$\alpha_{av} = \frac{1}{3} \sum \alpha_k \quad (4.1.31)$$

The nanoellipsoidal metallic particles are considered to be identical in composition, volume and shape then their corresponding semi major and minor axes, geometrical factors and polarizabilities are the same. Assuming diluted concentration of the particles we can use the Maxwell-Garnett formula for the effective dielectric function of the composite medium:

$$\epsilon = \epsilon_h \left(1 + \frac{f\alpha_{av}}{1 - fA_{av}}\right) \quad (4.1.32)$$

$$A_{av} = \frac{1}{3}(L_1\alpha_1 + L_2\alpha_2 + L_3\alpha_3) \quad (4.1.33)$$

The composite medium for very small filling factor of the particles, $f \ll 1$, terms with higher powers of f are negligible then the real and imaginary parts of the effective dielectric function of the medium are expressed by the following equations.

$$\epsilon_r = \left(1 + \frac{f\alpha_{avr}}{1 - 2fA_{avr}}\right)\epsilon_h \quad (4.1.34)$$

$$\epsilon_i = \frac{f\alpha_{avi}\epsilon_h}{1 - 2fA_{avr}} \quad (4.1.35)$$

$$\alpha_{avr} = \frac{1}{3}(\alpha_{1r} + \alpha_{2r} + \alpha_{3r}) \quad (4.1.36)$$

$$\alpha_{avi} = \frac{1}{3}(\alpha_{1ri} + \alpha_{2i} + \alpha_{3i}) \quad (4.1.37)$$

$$A_{avr} = \frac{1}{3}(L_1\alpha_{1r} + L_2\alpha_{2r} + L_3\alpha_{3r}) \quad (4.1.38)$$

$$A_{avi} = \frac{1}{3}(L_1\alpha_{1i} + L_2\alpha_{2i} + L_3\alpha_{3i}) \quad (4.1.39)$$

A general type of ellipsoid has unequal geometrical factors, $L_1 \neq L_2 \neq L_3$ for such type of ellipsoids it is more complicated to describe the effects of the different factors

on the polarizabilities and effective dielectric functions. For simplicity, in this study the particles are considered to be spheroids, spheroidal type ellipsoid has identical semi minor or major axes, for a prolate type spheroid $a > b = c$ and the geometrical factors with respect to the major and minor axes are, $L_1 \neq L_2 = L_3$ and related by [10]:

$$L_1 + 2L_2 = 1 \quad (4.1.40)$$

To a spheroid the changes in the geometrical factors are interrelated, the increase of the one encounters decrease of the other one as expressed by relation:

$$\Delta L_1 = -2\Delta L_2 \quad (4.1.41)$$

To randomly oriented spheroidal ellipsoids there are two resonance frequencies which are expressed by equation:

$$z_{Rk} = \frac{1}{\sqrt{\epsilon_\infty + (\frac{1}{L_k} - 1)\epsilon_h}} \quad (4.1.42)$$

where $k = 1, 2$ and the first and second resonance frequencies respectively are z_{r1} and z_{r2} , $z_{r1} \leq z_{r2}$ for $L_1 \leq L_2$. Equation (4.1.42) shows resonance frequency increases when its corresponding geometrical factor is increased.

Considering weakly damping case we can deduce the the variation of the real and imaginary parts of the polarizability and effective dielectric function with geometrical factor from the equations (4.1.26), (4.1.27) and (4.1.34)-(4.1.37). Both α_{avr} and ϵ_r show increase as L_1 increases in the range $L_1 > L_2$ and decrease as L_1 increases in the range $L_1 < L_2$. The effect of the geometrical factor on the imaginary parts is restricted in frequency intervals. In the interval $z > \frac{1}{\sqrt{\epsilon_\infty - \epsilon_h}}$, higher frequency region, α_{avi} and ϵ_i show the same variation as the real parts. And this effect is reversed in the interval $z < \frac{1}{\sqrt{\epsilon_\infty - \epsilon_h}}$, the frequency region considered in this study, in this interval α_{avi} and ϵ_i increase as L_1 increases in the range $L_1 < L_2$ and they are decreased as L_1 increases for $L_1 > L_2$.

We observe that both parts of the effective dielectric functions increase when concentration of the inclusions increases.

4.1.4 Refractive index in composite with pure metal ellipsoidal nanoparticles

The real and imaginary parts of the refractive index of a composite medium with pure metal ellipsoidal nanoinclusions are calculated from the effective dielectric functions using the equations (4.1.20) and (4.1.21) when the ellipsoids are aligned and equations (4.1.34) and (4.1.35) are used when the ellipsoids are randomly oriented in the passive host material the expressions for the real and imaginary parts of the refractive indexes are:

$$n_r = \sqrt{\frac{1}{2}(\epsilon_r + \sqrt{\epsilon_r^2 + \epsilon_i^2})} \quad (4.1.43)$$

$$n_i = \sqrt{\frac{1}{2}(-\epsilon_r + \sqrt{\epsilon_r^2 + \epsilon_i^2})} \quad (4.1.44)$$

With the help of the analysis in the previous sections we can show that both the maximum values to n_r and n_i will increase as the volume filling factor or concentration of the inclusions is increased for both cases. Equations (4.1.20) show that for the case of aligned ellipsoids the maximum value of n_r decrease when L_1 increases and from (4.1.34) and (4.1.35) it is observed that when nanometallic ellipsoids are randomly oriented the maximum value of n_r at a resonance frequency will increase when the geometrical factor which corresponds to the resonance frequency increases.

4.1.5 Group velocity of light pulses in the composite with with pure metal ellipsoidal nanoparticles

When all ellipsoidal particles are aligned and when they are randomly oriented in the passive dielectric material the group velocity is computed by using equation (4.1.43) into the equations (4.1.46) and (4.1.47).

$$v_g = \frac{\partial z}{\partial k}, \quad (4.1.45)$$

$$v_g = \frac{c}{n_g}, \quad (4.1.46)$$

$$n_g = n_r + z \frac{\partial n_r}{\partial z}, \quad (4.1.47)$$

4.2 Analytical description of refractive index and group velocity in composite with metal shell-dielectric core ellipsoidal nanoparticles

The polarizability of the metal covered dielectric particles depend on the dielectric properties of the core material, the metallic shell, and the host material and also on their geometrical factors and orientation. The equation for the polarizability that describes these dependences is derived in the same way as in the pure metal case based on electric potential distribution. Here we consider thickness of the metal shell to be small thus the confocal core and shell ellipsoids have nearly the same geometrical factors.

The electric potentials at different regions are expressed by the following equations [10]:

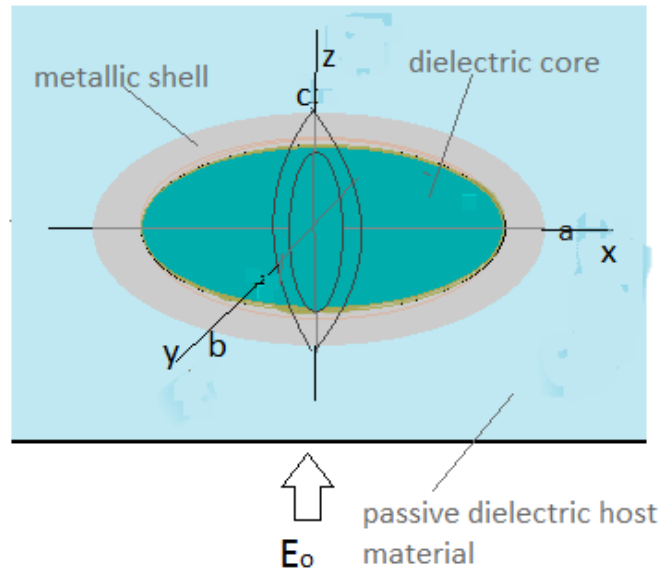


Figure 4.2: Metal shell-dielectric core nanoellipsoid embedded in passive dielectric host material

$$\phi_o = -E_o Z$$

$$\phi_d = A\phi_o \quad (4.2.1)$$

$$\phi_m = (B - CI_i)\phi_o \quad (4.2.2)$$

$$\phi_h = (1 - DI_o)\phi_o \quad (4.2.3)$$

$$\phi_p = DI_o\phi_o \quad (4.2.4)$$

$$I_i = \int_{\xi}^{\infty} \frac{dq}{(q + c_i^2)f(q)} \quad \text{and} \quad I_o = \int_{\xi}^{\infty} \frac{dq}{(q + c_o^2)f(q)} \quad (4.2.5)$$

where c_i and c_o are semi major axes respectively to the inner and outer ellipsoids, for a thin metal shell I and L are approximately the same to the inner and the outer ellipsoids. Applying the boundary conditions and equation for dipole moment in terms of polarizability α and applied field E_o equation for the polarizability can be derived as [10]:

$$\alpha = DI \quad (4.2.6)$$

$$\alpha = \frac{1}{L} \left(1 - \frac{u\epsilon_h}{w + (1-L)u\epsilon_h} \right) \quad (4.2.7)$$

$$u = \left(\frac{1}{Lp} - 1 \right) \epsilon_m + \epsilon_d \quad (4.2.8)$$

$$w = (1-L) \left(\epsilon_m^2 + \left(\frac{1}{p(1-L)} - 1 \right) \epsilon_d \epsilon_m \right) \quad (4.2.9)$$

where ϵ_d , ϵ_m and ϵ_h are respectively dielectric functions of the dielectric core, and the metal shell and the host matrix and p is the volume fraction of the metal shell in the ellipsoids.

4.2.1 When all metal shell-dielectric core ellipsoidal nanoparticles are aligned in passive dielectric material

The nanoellipsoidal particles are considered to be identical in composition, volume and shape, which are formed by confocal thin metal shell and dielectric core. In this case all particles are aligned like the particles in section 4.1 and their concentration is very small. The dielectric function of the dielectric core ϵ_d is taken to be real positive and for the metal shell ϵ_m is in Drude form. The electric field is applied parallel to a principal axis of the aligned inclusions. The effective polarizability of the inclusions that corresponds to this principal axes can be expressed by relation [10, 11];

$$\alpha = \frac{1}{L} - \frac{h}{b} \quad (4.2.10)$$

$$h = \frac{1}{L(1-L)} \left(\frac{\epsilon_m}{Lp} + \epsilon_d \right) \epsilon_h \quad (4.2.11)$$

$$b = \epsilon_m^2 + q\epsilon_m + \epsilon_d\epsilon_h \quad (4.2.12)$$

$$q = \frac{\epsilon_d}{p(1-L)} + \frac{\epsilon_h}{pL} \quad (4.2.13)$$

where p is assumed to be small i.e $p \ll 1$ and L is geometrical factor with respect to the axes of the ellipsoid which is considered to be parallel to the polarizing field. We observe in equation (4.2.13) q is a real value. The real and imaginary parts of h , b and α are respectively expressed by;

$$h_r = \frac{1}{L(1-L)} \left(\frac{\epsilon_{mr}}{pL} + \epsilon_d \right) \epsilon_h \quad (4.2.14)$$

$$h_i = \frac{\epsilon_h \epsilon_{mi}}{pL^2(1-L)} \quad (4.2.15)$$

$$b_r = \epsilon_{mr}^2 + q\epsilon_{mr} + \epsilon_d\epsilon_h - \epsilon_{mi}^2 \quad (4.2.16)$$

$$b_i = (2\epsilon_{mr} + q)\epsilon_{mi} \quad (4.2.17)$$

$$q = \frac{\epsilon_d}{p(1-L)} + \frac{\epsilon_h}{pL} \quad (4.2.18)$$

$$\alpha_r = \frac{1}{L} + \frac{h_i b_i - h_r b_r}{b_r^2 + b_i^2} \quad (4.2.19)$$

$$\alpha_i = \frac{h_i b_r - h_r b_i}{b_r^2 + b_i^2} \quad (4.2.20)$$

The polarizability and dielectric function can be analyzed by assuming very weak damping of plasma in the metal part, i.e $\gamma \ll 1$ then about frequencies close to plasma frequencies $\epsilon_{mi} \ll 1$. The resonance condition is obtained from the minimum of equations (4.2.19) and (4.1.20) this happens when $b_r = 0$ and this leads to the equation;

$$\epsilon_{mr}^2 + q\epsilon_{mr} + \epsilon_d\epsilon_h = 0 \quad (4.2.21)$$

Equation (4.2.21) has two roots for the real part of dielectric function of the metallic shell. Considering that $q \gg \epsilon_d\epsilon_h$ the first and the second roots are respectively approximated by the following relations

$$\epsilon_{mr1} = -q \quad (4.2.22)$$

$$\epsilon_{mr2} = -\frac{\epsilon_d \epsilon_h}{q} \quad (4.2.23)$$

Then using equation (4.1.6) the corresponding two resonance frequencies are given by the equations

$$z_{R1} = \frac{1}{\sqrt{\epsilon_\infty + q}} \quad (4.2.24)$$

$$z_{R2} = \frac{1}{\sqrt{\epsilon_\infty}} \quad (4.2.25)$$

From the above equations it is observed that the geometrical factor L and the metal volume fraction p of inclusions affect significantly the first resonance frequency z_{R1} but their effect is very small on the second one so z_{R2} seems to be fixed point. z_{R1} increases when p increases and also increase when L is increased up to the limiting value about 0.5223 when L is increased above this value z_{R1} will decrease. The real and the imaginary parts of the polarizability at the resonance frequencies are determined from equations (4.2.10)-(4.2.20) and thin metal shell approximation, $p \ll 1$.

$$\alpha_r(z_{R1}) \approx \frac{\epsilon_d - \epsilon_h}{\epsilon_h + L[\epsilon_d - \epsilon_h]} \quad (4.2.26)$$

$$\alpha_i(z_{R1}) \approx -\frac{\epsilon_h}{pL^2(1-L)\epsilon_{mi}} \quad (4.2.27)$$

$$\alpha_r(z_{R2}) \approx \frac{\epsilon_d}{\epsilon_h + L\epsilon_d} \quad (4.2.28)$$

$$\alpha_i(z_{R2}) \approx -\frac{pL\epsilon_d^2\epsilon_h}{(\epsilon_h + L(\epsilon_d - \epsilon_h))^2\epsilon_{mi}} \quad (4.2.29)$$

Effective DF of the composite in this case is expressed by the same equation as the case with aligned pure metal inclusions, equations (4.1.20) and (4.1.21), the real and imaginary effective dielectric functions for the dilute concentration of the ellipsoidal metal covered dielectric nanoparticles can be:

$$\epsilon_r = \left(1 + \frac{f\alpha_r}{1 - 2fL\alpha_r}\right)\epsilon_h \quad (4.2.30)$$

$$\epsilon_i = \frac{f\alpha_i\epsilon_h}{1 - 2fL\alpha_r} \quad (4.2.31)$$

4.2.2 When the metal shell-dielectric core ellipsoidal nanoparticles are randomly oriented in passive dielectric material

In this case we use the same equations and considerations as in the case of randomly distributed pure metallic inclusions, but here the dielectric function of the metallic shell ϵ_m and the dielectric function of the dielectric core ϵ_d are considered for the composite ellipsoidal particles. The relations for polarizabilities to the aligned metal shell-dielectric core particles are generalized for the randomly distributed ones by inserting subscript k to denote one of the three alternate principal axes directions and real and imaginary parts of polarizability with respect to the k^{th} , $k = 1, 2, 3$, principal axes are given by:

$$\alpha_{kr} = \frac{1}{L_k} + \frac{h_{ki}b_{kr} - h_{kr}b_{ki}}{b_{kr}^2 + b_{ki}^2}, \quad (4.2.32)$$

$$\alpha_{ki} = \frac{h_{ki}b_{kr} - h_{kr}b_{ki}}{b_{kr}^2 + b_{ki}^2}, \quad (4.2.33)$$

$$h_{kr} = \frac{\epsilon_h}{L_k(1 - L_k)} \left(\frac{\epsilon_{mr}}{pL_k} + \epsilon_d \right), \quad (4.2.34)$$

$$h_{ki} = \frac{\epsilon_h \epsilon_{mi}}{pL_k^2(1 - L_k)}, \quad (4.2.35)$$

$$b_{kr} = \epsilon_{mr}^2 + q_k \epsilon_{mr} + \epsilon_d \epsilon_h - \epsilon_{mi}^2, \quad (4.2.36)$$

$$b_{ki} = (2\epsilon_{mr} + q_k) \epsilon_{mi}, \quad (4.2.37)$$

$$q_k = \frac{\epsilon_d}{p(1 - L_k)} + \frac{\epsilon_h}{pL_k}. \quad (4.2.38)$$

Following the same procedure as in the previous section for resonance condition $b_{kr}=0$ is required then for small damping case this is obtained from the equations (4.2.32)-(4.2.33) as:

$$\epsilon_{mr}^2 + q_k \epsilon_{mr} + \epsilon_d \epsilon_h = 0 \quad (4.2.39)$$

It is shown that for general type ellipsoids, which have unequal semi minor and major axes, there are two roots of equation (4.2.39) to each of the three principal axes and totally there are six roots hence there can be up to six resonance frequencies which are given by two set of relations each representing three resonance frequencies:

$$z_{kRa} = \frac{1}{\sqrt{\epsilon_\infty + q_k}}, \quad (4.2.40)$$

$$z_{kRb} = \frac{1}{\sqrt{\epsilon_\infty + \frac{\epsilon_d \epsilon_h}{q_k}}}, \quad (4.2.41)$$

since $\frac{\epsilon_d \epsilon_h}{q_k} \ll \epsilon_\infty$ the second equation can be approximated to

$$z_{kRb} \approx \frac{1}{\sqrt{\epsilon_\infty}} \quad (4.2.42)$$

Equation (4.2.42) shows that the different k directions have approximately the same resonance frequency z_{kRb} . In this case the inclusions are considered to be identical spheroids then $k = 1, 2$ and $L_1 + 2L_2 = 1$. Actually there are two resonance frequencies z_{kRa} . But from equations (4.2.40) and (4.2.38) we deduced that the two resonance frequencies differ by a very small amount, $\propto 10^{-3}$ and less, for this reason they are not distinguishable. Hence to this composite only two resonance frequencies are significantly observable.

4.2.3 Effective dielectric function of the composite medium

The relations for the effective dielectric function as well as its real and imaginary parts are expressed by the following equations

$$\epsilon = \left(1 + \frac{f\alpha_{av}}{1 - fA_{av}}\right)\epsilon_h, \quad (4.2.43)$$

$$\epsilon_r = \left(1 + \frac{f\alpha_{avr}}{1 - 2fA_{avr}}\right)\epsilon_h, \quad (4.2.44)$$

$$\epsilon_i = \frac{f\alpha_{avi}\epsilon_h}{1 - 2fA_{avr}}, \quad (4.2.45)$$

$$\alpha_{avr} = \frac{1}{3}(\alpha_{1r} + \alpha_{2r} + \alpha_{3r}), \quad (4.2.46)$$

$$\alpha_{avi} = \frac{1}{3}(\alpha_{1i} + \alpha_{2i} + \alpha_{3i}), \quad (4.2.47)$$

$$A_{avr} = \frac{1}{3}(L_1\alpha_{1r} + L_2\alpha_{2r} + L_3\alpha_{3r}), \quad (4.2.48)$$

where A_{avr} is the real part of A_{av} .

4.2.4 Refractive index of the composite medium

The real and imaginary parts of the refractive index of the composite medium with metal-shell dielectric core nanoellipsoids are given by the same equations as in the composite with pure metal inclusions. Equations (4.2.30)-(4.2.31) can be used to composites with aligned nanoellipsoids and (4.2.44) and (4.2.45) are applied to composites with randomly oriented nanoellipsoids to compute real and imaginary parts of the refractive index in the medium

$$n_r = \sqrt{\frac{1}{2}(\epsilon_r + \sqrt{\epsilon_r^2 + \epsilon_i^2})}, \quad (4.2.49)$$

$$n_i = \sqrt{\frac{1}{2}(-\epsilon_r + \sqrt{\epsilon_r^2 + \epsilon_i^2})}. \quad (4.2.50)$$

4.2.5 Group velocity in the composite with ellipsoidal metal shell-dielectric core nanoparticles

The group velocity is calculated using the equations for the real refractive index (4.2.49) with the equation

$$v_g = \frac{c}{n_r + z \frac{\partial n_r}{\partial z}} \quad (4.2.51)$$

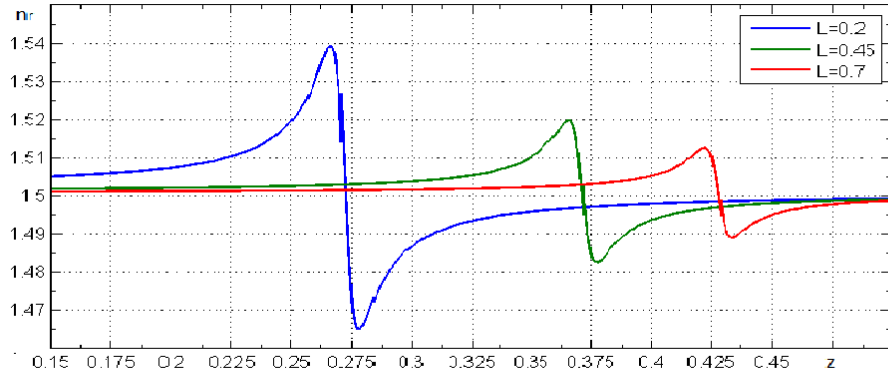
From equation (4.2.51) we conclude that group velocity get its maximum value at frequency where real part of the refractive index is minimum value, and become minimum value at resonance frequency where the real part of the refractive index is maximum. Group velocity can be positive and decreases in the frequency interval of normal dispersion, $\frac{\partial n_r}{\partial z} > 0$, and it can be positive and decreasing or negative and decreasing in the frequency interval of anomalous dispersion, $\frac{\partial n_r}{\partial z} < 0$. In the anomalous dispersion region at frequencies where the group velocity index $|n_g| < 1$, group velocity has positive or negative value which exceed the speed of light in free space this virtual case is referred as superluminal light.

4.3 Numerical description of refractive index in composite with ellipsoidal pure metal nanoparticles

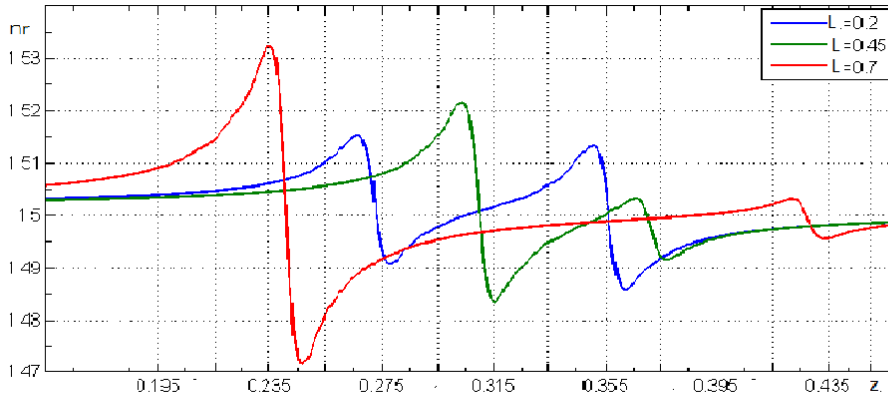
The numerical computation of the variation of real part of the refractive index with geometrical factor and concentration of nanometallic inclusions is carried out using the equation (4.1.43) with equations (4.1.20) and (4.1.21) for the case when all inclusions are aligned and equations (4.1.34) and (4.1.35) for the case when the inclusions are randomly oriented in the passive dielectric material and the results are plotted in figures 4.3-4.4 using the following parameters for all cases; $\epsilon_\infty = 4.5$, $\epsilon_h = 2.25$, $\epsilon_d = 6$, $\gamma = 0.0115$, $\omega_p = 1.46 \times 10^{16} \frac{rad}{s}$ for silver.

4.3.1 The effect of geometrical factor of the ellipsoidal pure metal nanoparticles on the refractive index

Figures 4.3 illustrate the variation of real part of refractive index with frequency of the incident light for different values of the geometrical factor. We observe that for the case when the pure metal nanoellipsoids are aligned there is a single resonance frequency. There are two resonance frequencies for the case when they are randomly oriented. In both cases resonance frequency increases, shifted to the right, when the corresponding geometrical factor increased and it decreases when the geometrical factor decreased. But when geometrical factor increased the maximum value of the real part of refractive index shows a decrease and its minimum value shows an increase.



(a)



(b)

Figure 4.3: The real part of the refractive index n_r versus frequency z of applied field for three geometrical factors when the pure metal nanoellipsoids are aligned part (a) and randomly oriented part (b) in passive dielectric material with concentration $f = 0.001$

4.3.2 Effect of the concentration of the ellipsoidal metallic nanoparticles in the composite on the refractive index

Figures 4.4 illustrate how the concentration of the nanometallic ellipsoids affect the real part of the refractive index in the composites. In the figure 4.4(a) the real part of the refractive index increases with the increasing concentration of the aligned metallic nanoellipsoids to frequencies $z < 0.273$ and it decreases to the frequencies $z > 0.273$. In the figure 4.4(b) to the composite with randomly oriented metallic nanoellipsoids the refractive index increases with the increasing concentration of inclusions in the intervals $z < 0.273$ and $0.305 < z < 0.355$ but it decreases with the increasing concentration in

the regions $0.273 < z < 0.305$ and $z > 0.355$. For both cases the resonance frequencies where the refractive index is maximum and the frequencies where refractive index is minimum remain the same for the different concentrations of the inclusions, but the peak value of refractive index increases while its minimum value decreases with the increasing concentration.

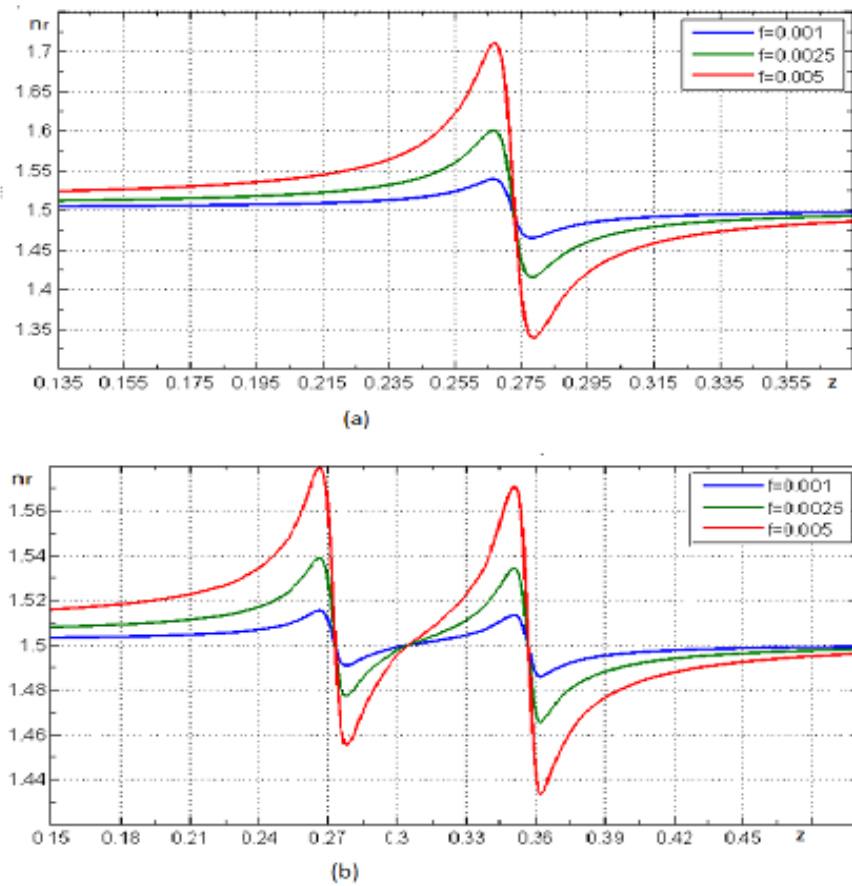


Figure 4.4: The real part of refractive index n_r versus frequency of applied field z for three values volume filling factor of the pure metal nanoellipsoidal inclusions embedded in passive dielectric material with geometrical factor $L = 0.2$, part (a) is when the ellipsoids are aligned and part (b) is when they are randomly oriented

4.4 Numerical description of refractive index in composite with ellipsoidal metal shell-dielectric core nanoparticles

The numerical description of the effect on the real part of refractive index by the geometrical factor and concentration of metal covered dielectric core inclusions in passive dielectric material is computed using equations (4.2.50) and (4.2.19) and (4.2.20) with equations (4.2.30) and (4.2.31) for the case when inclusions are aligned and equations (4.2.44) and (4.2.45) for the case when they are randomly oriented.

The dielectric function of the dielectric core is chosen to be real, $\epsilon_d = 6$, the volume fraction of the metal in the ellipsoidal inclusion $p = 0.1$ and the same values are used for the parameters used in the previous section.

4.4.1 The effect of geometrical factor of the ellipsoidal metal shell-dielectric core nanoparticles on the refractive index

As shown in the figures 4.5 both cases have the same resonance frequencies and the effect on the second resonance frequency by the geometrical factor is vary small, not observable, but there is slight shift of the first resonance frequency with the geometrical factor. With the increase of the geometrical factor the maximum of the real part of refractive index shows decrease in aligned nanoellipsoids and it show increase in randomly oriented nanoellipsoids. After the first resonance frequency there is an interval for anomalous dispersion where the refractive index decreases to minimum value. This minimum value increase with the geometrical factor in composite with aligned nanoellipsoids, and it decreases with the increase of the geometrical factor in the composite of randomly oriented nanoellipsoids.

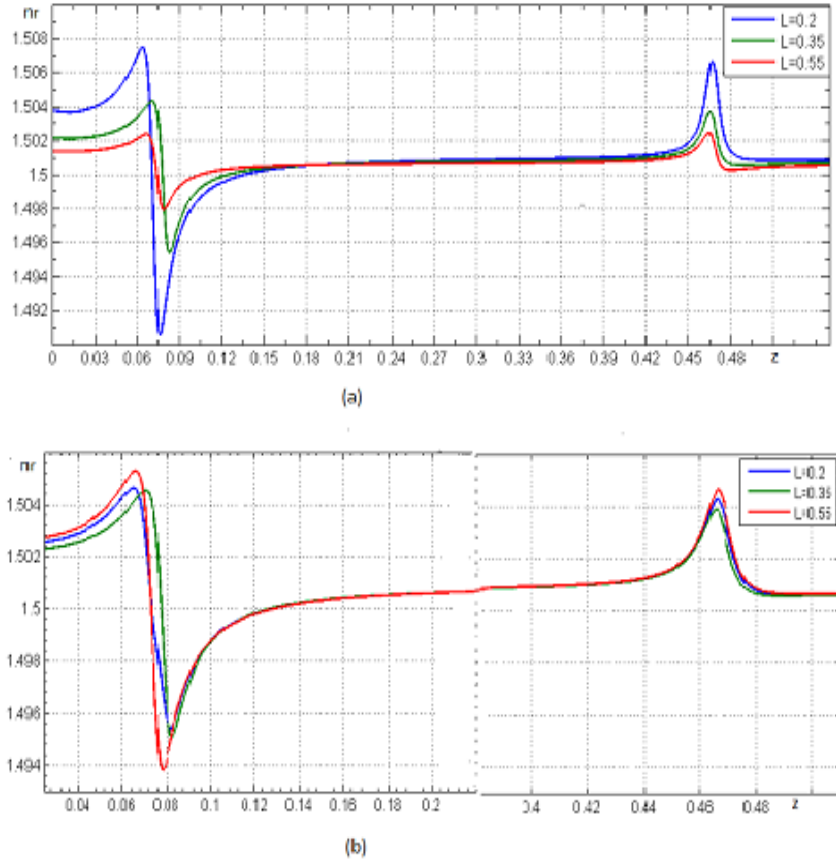


Figure 4.5: The real part of refractive index n_r versus applied field frequency z for three values of geometrical factor in composite with metal shell-dielectric core nanoellipsoids embedded in passive materia with concentration $f = 0.001$ and volume fraction of the metal part in the ellipsoids $p = 0.1$, part (a) is when the ellipsoids are aligned and part (b) is when they are randomly oriented

4.4.2 The effect of the concentration of the ellipsoidal metal shell-dielectric core nanoparticles on the refractive index

In the figures 4.6 we observe that resonance frequencies are the same for the two cases and in both cases the real part of the refractive index increases as the concentration of nanoellipsods increase. The differences in the two cases are the peak values of the refractive index are greater for the aligned nanoellipsods case than the corresponding values in the case of randomly oriented ellipsoids. The minimum value of the refractive

index in the case of aligned ellipsoids is less than the corresponding minimum value in randomly oriented nanoellipsoids.

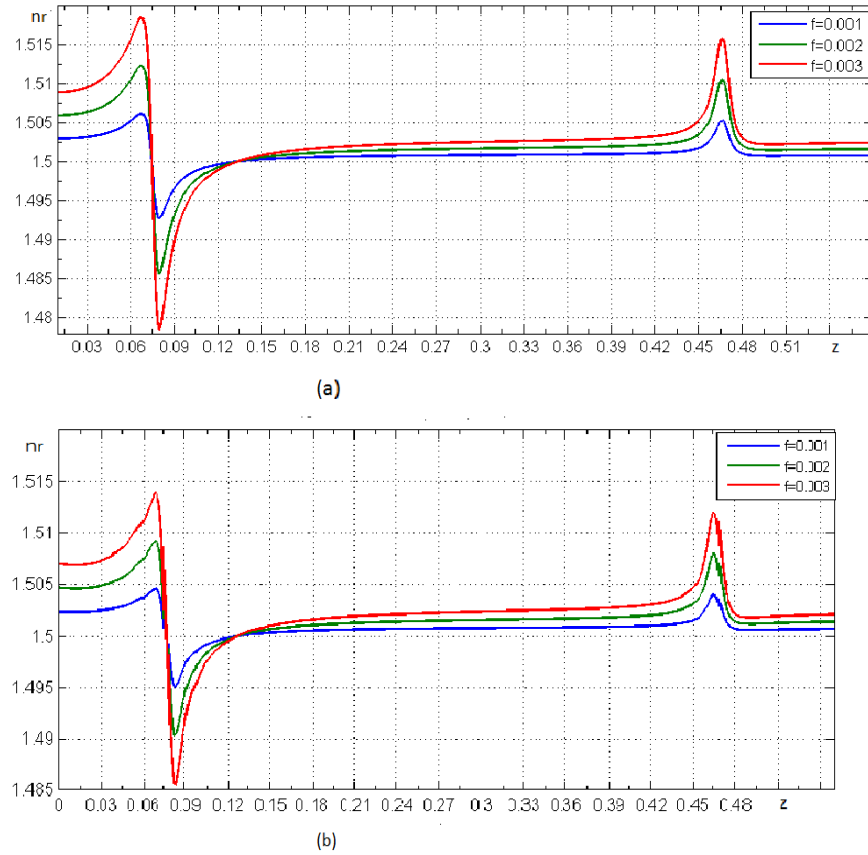


Figure 4.6: The real part of refractive index n_r versus applied field frequency z for three values of concentration of metal shell-dielectric core nanoellipsoids embedded in passive dielectric material with geometrical factor $L = 0.25$ and $p = 0.1$, part (a) is for aligned ellipsoids case and part (b) is for the randomly oriented ellipsoids case

4.4.3 **The effect of the metal volume fraction in the metal shell-dielectric core nanoparticles on the refractive index**

In the figures 4.7 we observe that resonance frequencies are the same in the two cases. In both cases, the real part of the refractive index increases as the concentration of nanoellipsoids increase. The differences in the two cases are peak values of the refractive index are greater for the aligned nanoellipsoids case than the corresponding values in the case of randomly oriented ellipsoids, and minimum value of the refractive index in the case of aligned ellipsoids is less than the corresponding minimum value in randomly oriented nanoellipsoids.

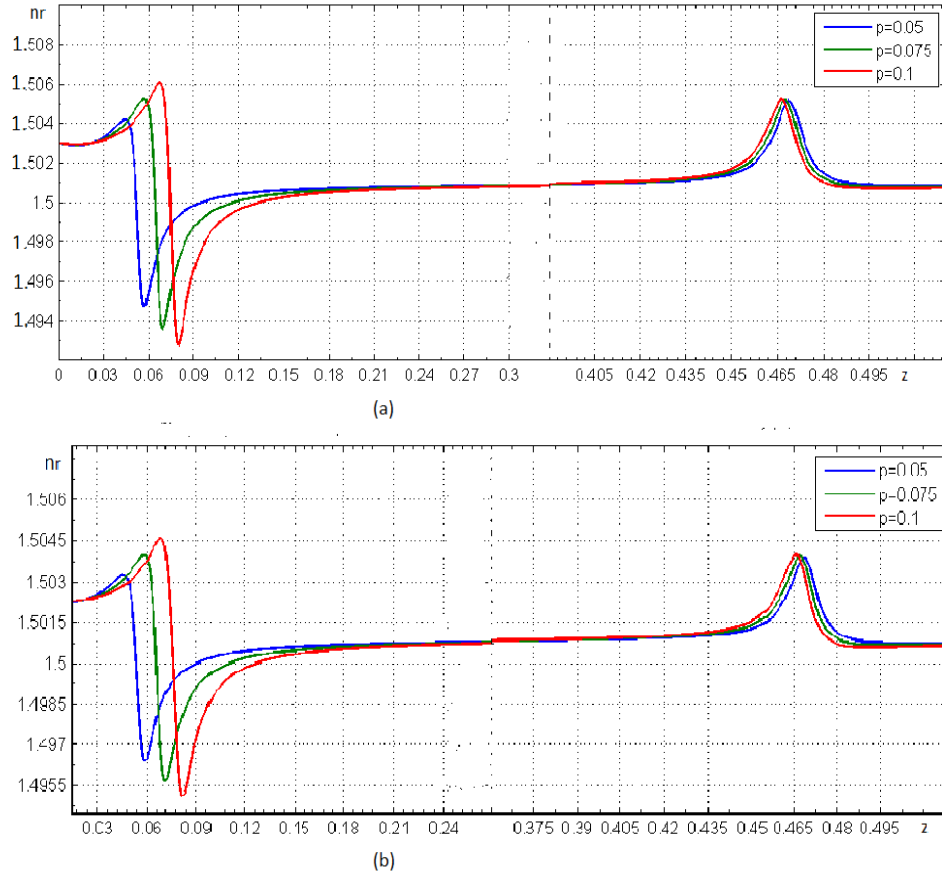


Figure 4.7: The real part of refractive index n_r versus applied field frequency z for three values of the metal volume fraction in the metal shell-dielectric core nanoellipsoids with geometrical factor $L = 0.25$ and their concentration $f = 0.001$ in passive material, parts a and b are respectively when the nanoellipsoidal inclusions are aligned and randomly oriented

4.5 Numerical description of group velocity in composite with ellipsoidal pure nanoparticles

The effects of geometrical factor and concentration of ellipsoidal pure metal nanoparticles on group velocity is analyzed numerically with the help of equations (4.1.43) with (4.1.47) and (4.2.49) with (4.2.50) and the results are plotted as shown in the figures 4.8-12. the parameters used as constant values in previous section considered again in this section.

4.5.1 The effect of the geometrical factor of the ellipsoidal pure metal nanoparticles on group velocity

The figures 4.8 describe effect of the geometrical factor on the group velocity in composite with ellipsoidal pure metal nanoparticles. Concentration of the ellipsoidal metallic nanoparticles is considered to be vary dilute, $f = 0.001$, in the figures it is shown that $0 < v_g/c < 1$ to all frequencies thus both cases describe light propagating to the forward at group velocity below the speed of light in free space. An increase in the geometrical factor associated to a resonance frequency causes increase of the peak value of group velocity about that resonance frequency for both cases.

The main differenc due to single resonance condition in aligned metallic nanoellipsoids the resulting frequency at which group velocity is peaked is one but in randomly oriented metallic nanoellipsoids there are two resonance points. The group velocity is observed to peak at two frequencies in the randomly oriented ellipsoids. The peak value of group velocity in aligned nanoellipsoids is greater than the corresponding peak value in randomly oriented nanoellipsoids. Thus the composites with aligned metallic nanoellipsoids allow transmission of forward light pulses at resonance frequency at greater speed than that in the randomly oriented metallic nanoellipsoids.

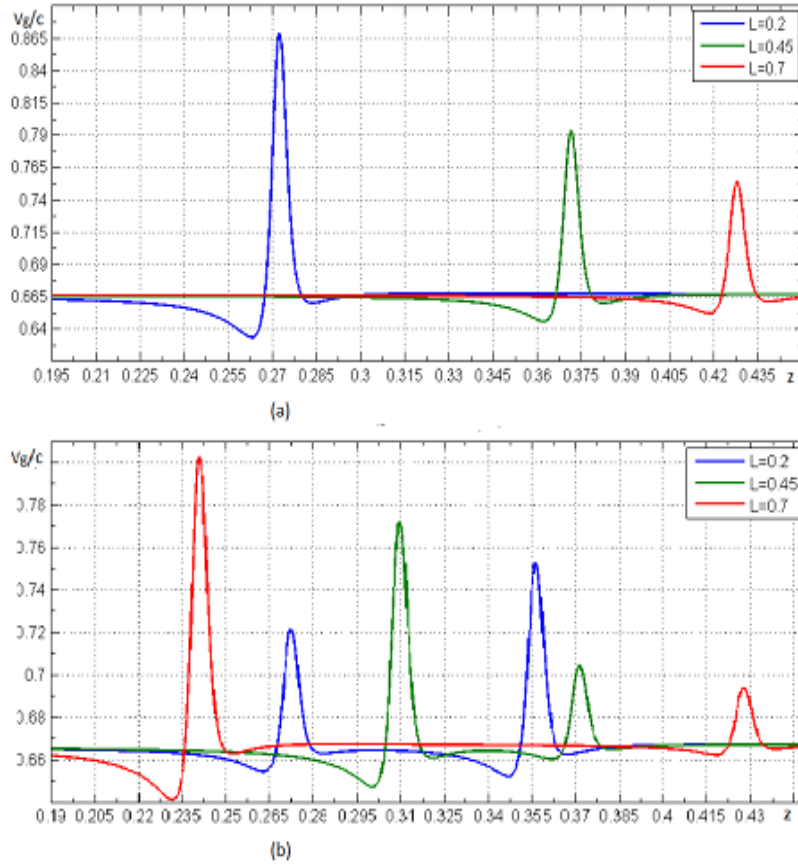


Figure 4.8: Group velocity normalized to speed of light in free space $\frac{v}{c}$ versus applied field frequency z in composite with pure metal nanoellipsoids for three geometrical factor values. concentration of the ellipsoids $f = 0.001$ respectively parts (a) and (b) are when the ellipsoids are aligned and randomly oriented in the passive material

4.5.2 The effect of concentration of ellipsoidal pure metal nanoparticles on the group velocity

As shown in the figures 4.9 increase in concentration of the ellipsoidal metallic nanoparticles increases the group velocity and its peak value in the anomalous dispersion region, and decrease group velocity and its minimum in the region of normal dispersion. In the anomalous region it is seen $v_g > 1$ for higher concentrations in both cases. Group velocity increase in anomalous region with concentration of nanometal ellipsoids more in aligned nanoellipsoids case than in the randomly nanoellipsoids case. The peak value of group

velocity is greater in the case of aligned ellipsoids than the value in the case of randomly oriented ellipsoids.

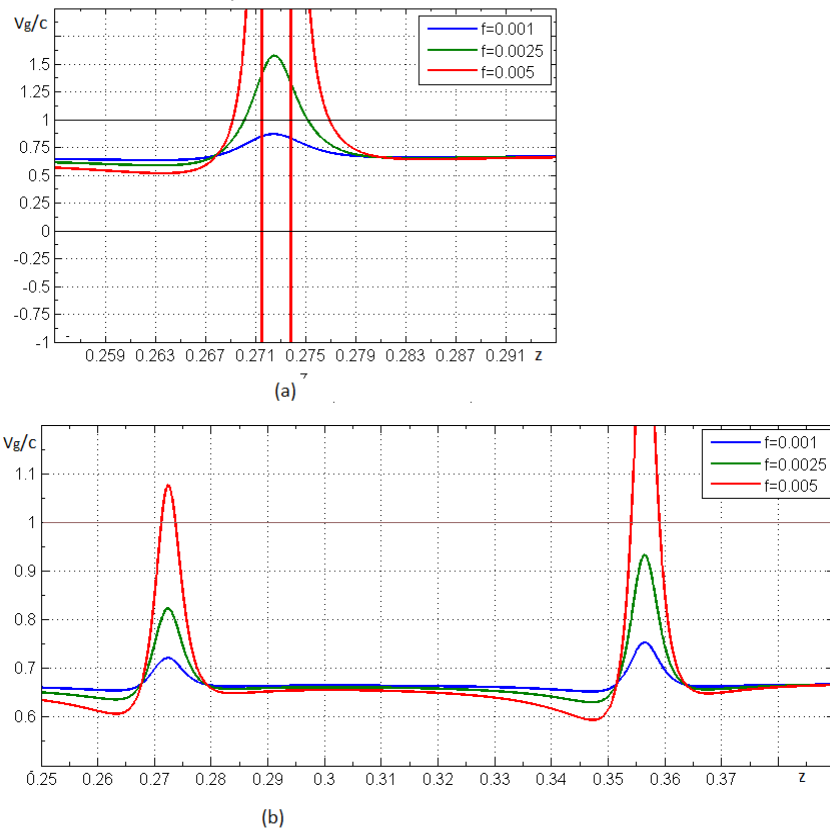


Figure 4.9: Group velocity to speed of light in free space $\frac{v}{c}$ versus applied field frequency z in composite with pure metal nanoellipsoids for three values of their concentration and their geometrical factor $L = 0.2$, respectively parts (a) and (b) are when the ellipsoids are aligned and randomly oriented in the passive material

4.6 Numerical description of group velocity in composite with metal shell-dielectric core ellipsoidal nanoparticles

The group velocity of light pulses in composite with metal shell-dielectric core nanoellipsoids embedded in passive material can be analyzed numerically using equations for the effective dielectric functions for the medium and and equations (4.2.49) and (4.2.50).

4.6.1 The effect of the geometrical factor of the metal shell-dielectric core ellipsoidal nanoparticles on the group velocity in composite

The figures 4.10 illustrate how the variation of group velocity with frequency is changed with the changing geometrical factor. In both cases; the aligned and randomly oriented inclusions, group velocity is minimum at resonance frequencies and maximum at the end of the anomalous region. Between the peak values group velocity has nearly uniform value in the intermediate region, $0.12 \leq z \leq 0.43$. The frequencies at which group velocity be minimum and maximum are affected by the change in geometrical factor in the same way as mentioned in section 4.5.1.

With the increasing geometrical factor the observed differences between the two cases are, in composite with aligned inclusions the minimum value of the group velocity increases while its maximum decreases at the two resonance points, in composite with randomly oriented inclusions at first resonance frequency the minimum value of the group velocity decreases and its peak value increases. At the second resonance frequency the minimum value of group velocity increases while its peak value decreases with the increasing geometrical factor from zero up to 0.5223. For the increase in the geometrical factor beyond 0.5223 the minimum value decreases while the peak value increase.

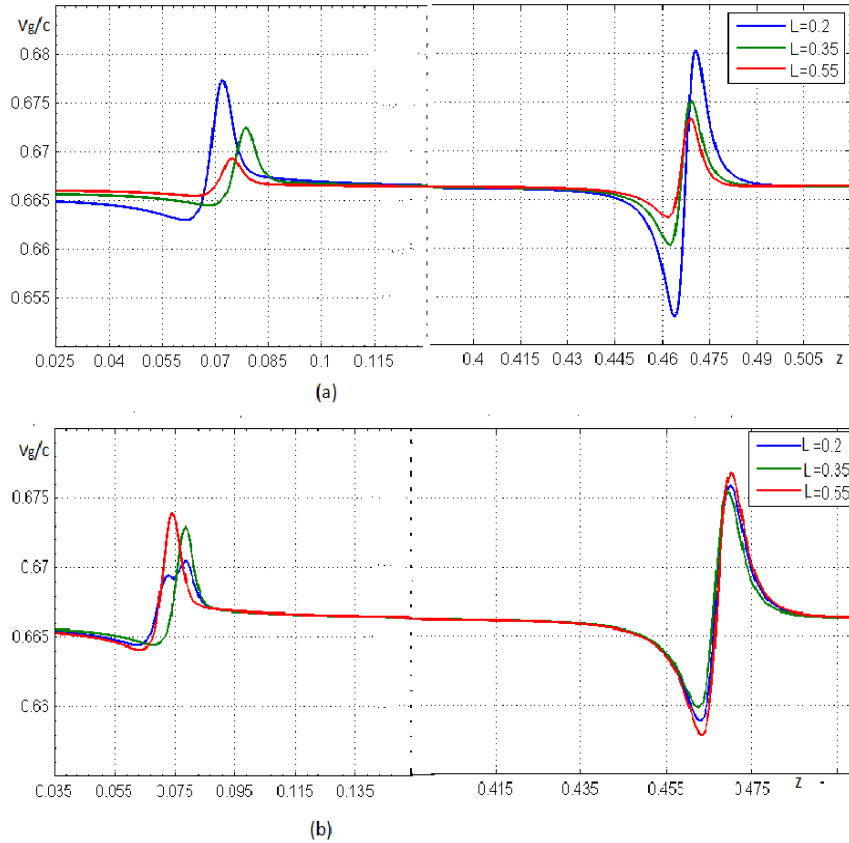


Figure 4.10: Group velocity to speed of light in free space $\frac{v_g}{c}$ versus applied field frequency z in composite with metal shell-dielectric core nanoellipsoids for three geometrical factor values. concentration of the nanoellipsoids $f = 0.001$ and volume fraction of metal part $p = 0.1$, respectively parts (a) and (b) are when the ellipsoids are aligned and randomly oriented in the passive material

4.6.2 The effect of concentration of metal shell-dielectric core ellipsoidal nanoparticles on the group velocity

The changes in group velocity with the change of the concentration of the aligned and randomly oriented ellipsoidal metal shell-dielectric core nanoparticles are illustrated respectively in the figures 4.10 (a) and (b). It is observed that in both cases the effect of concentration of inclusions on the group velocity is the same. At low frequencies up to the first resonance frequency, and about the second resonance frequency group velocity decreases when the concentration of the inclusions increases. Peak values of the group

velocity at both resonance points increases when the concentration increase.

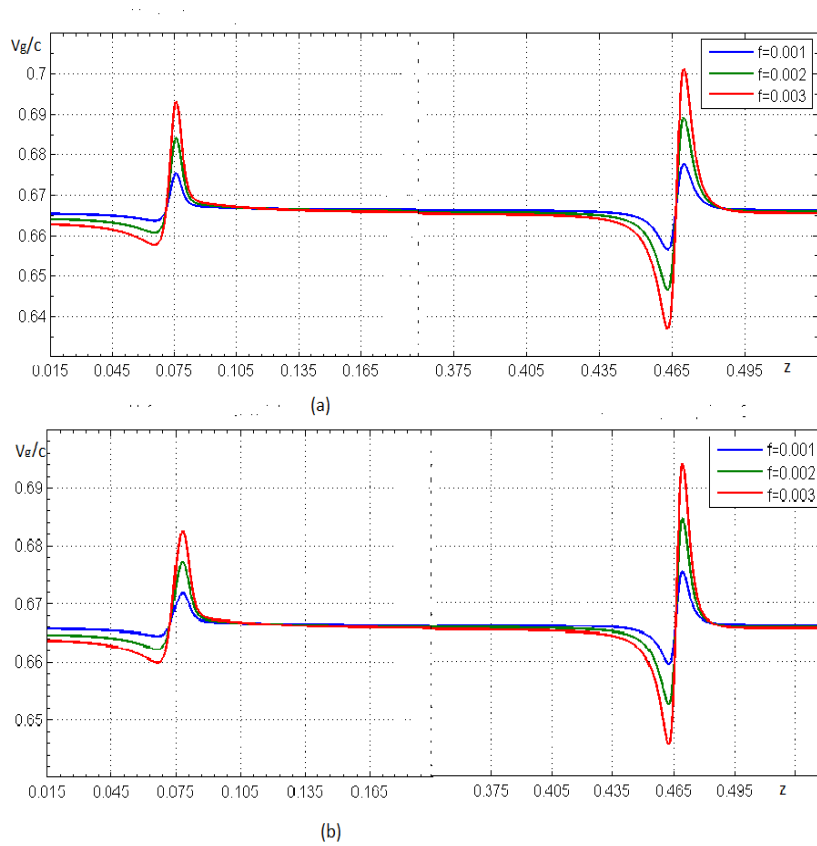


Figure 4.11: Group velocity to speed of light in free space $\frac{v}{c}$ versus applied field frequency z in composite with metal-shell dielectric core nanoellipsoids for three values of their concentration, with geometrical factor $L = 0.25$ and the metal fraction $p = 0.1$, respectively parts (a) and (b) are when the ellipsoids are aligned and randomly oriented in the passive material

4.6.3 The effect of metal volume fraction in the metal shell-dielectric core ellipsoidal nanoparticles on group velocity

In composites with metal shell-dielectric core ellipsoidal nanoparticles the effects on the group velocity by the volume fraction of the metal part are illustrated in the figures 4.12(a) and (b). with increase in volume fraction of the metal part there is significant increase of the first resonance frequency and vary small (insignificant) decrease of the second resonance frequency. An increase in the volume fraction of the metal part causes a significant increase of the peak value of group velocity, and a decrease of its minimum value at first resonance frequency. And increases the peak and minimum values of the group velocity at the second resonance frequency.

The differences between the two cases are peak values of group velocities in the case of aligned inclusions is greater than the corresponding peak values in randomly oriented inclusions. And in aligned inclusions the minimum value of group velocity is smaller than the corresponding minimum values in randomly oriented inclusions.

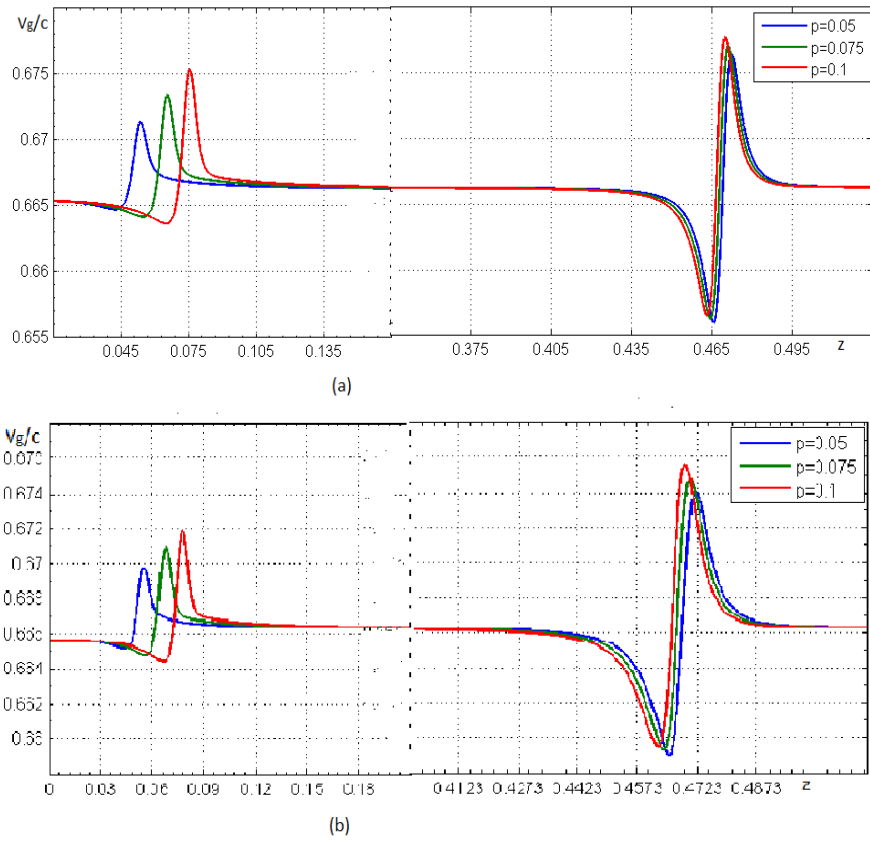


Figure 4.12: Group velocity to speed of light in free space $\frac{v_g}{c}$ versus applied field frequency z in composite with metal-shell dielectric core nanoellipsoids for three values of the metal volume fraction in the ellipsoids with geometrical factor $L = 0.25$ and concentration $f = 0.001$, respectively parts (a) and (b) are when the ellipsoids are aligned and randomly oriented in the passive material

Chapter 5

Conclusion and future outlook

In this study we focused on composite medium consisting identical inclusions which are nanoellipsoids embedded in passive dielectric material. To the inclusions of pure metal and metal covered dielectric core types the cases when all aligned and when they are randomly oriented are considered. The concentration of the inclusions in the composite is chosen to be dilute, $f \sim 10^{-3}$.

The effects on the real part of the refractive index and the group velocity of the wave packets in the composite due to the changes in the geometrical factor, fraction of metal part and concentration of inclusions computed and analyzed for the different cases are shown in the figures 4.3 - 4.12 and we have compared the results between aligned and randomly oriented inclusions of the same type and between different types of inclusions with the same arrangement.

As we have seen in all the cases considered in this study the concentration of the nanoellipsoidal inclusions in the composites has considerable effect on the maximum and minimum values of the refractive index and the group velocity but it doesn't change the resonance frequencies.

The geometrical factor of the nanoellipsodal inclusions determine the resonance frequencies and maximum and minimum values of the refractive index and the group velocity. In the case of pure metal ellipsoids and aligned metal covered dielectric core ellipsoids the observed effects of the geometrical factor are comparable at both resonance frequencies

but in the case of randomly oriented metal covered dielectric core nanoellipsoids considerable effect of geometrical factor is observed at the first resonance frequency at the second one its effect is vary small. Similarly the metal volume fraction in metal covered dielectric core ellipsoids has observable effect on the resonance frequency, maximum and minimum values of refractive index and group velocity at the first resonance frequency. But its effect is vary weak at the second resonance frequency.

We have seen also the effects caused by the orientation, to be aligned or randomness, of the ellipsoids; in the case of pure metal inclusions their orientation determines the number of resonance frequencies as well as the maximum and minimum values of the refractive index and the group velocity but in the case of metal covered dielectric core inclusions which has two distinctly observable resonance frequencies for both types of orientations the orientation of inclusions determine the effect resulting by the geometrical factor.

Nanometal/dielectric composites are needed for different applications which require a frequency range for operation and efficient transmission of light, these important properties are obtained by properly designing the nanoparticles composition, size, concentration, orientation and the nature of embedding material as tuning options.

The composites with pure metal nanoellipsoids provide the options; the geometrical factor, concentration and orientation of the ellipsoids to tune the composite for the required purpose but the composites with metal covered dielectric core nanoellipsoids have additional options, the volume fraction of the metal part in the ellipsoids and dielectric function of the dielectric core.

Unlike the pure metal nanoellipsoids the metal covered dielectric core nanoellipsoids provide a nearly fixed second resonance frequency while the first one is adjustable for the required range.

The increase in concentration of pure metal ellipsoids may lead to superluminal light and results high absorption and lose. This effect is observed in the composite of metal covered

dielectric core ellipsoids at higher concentration limit than that in the pure metal case.

Future plane is to investigate about the imaginary part of refractive index and absorption in medium with ellipsoidal metal/dielectric composite nanoparticles. And studying about refractive index, propagation and absorption of light in a medium with ellipsoidal metal/dielectric composite nanoparticles embedded in active medium including the influence of dielectric nature of the dielectric core.

Bibliography

- [1] D. Hull. An Introduction to Composite Materials. *Journal of Mechanical Working Technology*, 7(1):298–299, 1983.
- [2] J. Pérez-Juste, B. Rodríguez-González, P. Mulvaney, and L. M. Liz-Marzán. Optical Control and Patterning of Gold-Nanorod-Poly(vinyl alcohol) Nanocomposite Films. *Advanced Functional Materials*, 15(7):1065–1071, 2005.
- [3] W. L. Barnes, A. Dereux, and T. W. Ebbesen. Surface plasmon subwavelength optics. *Nature*, 424(6950):824–30, 2003.
- [4] C. Noguez. Surface Plasmons on Metal Nanoparticles: The Influence of Shape and Physical Environment. *Journal of Physical Chemistry C*, 111(10):3806–3819, 2007.
- [5] M. Standtke and L. Kuipers. slow guided surface plasmons at telecom frequencies. *Nat. Photonics*, 1 (10):573–576, 2007.
- [6] V.E. Ferry L.A. Sweatlock D. Pacifici and H.A. Atwater. plasmonic nanostructure design for efficient light coupling in to solar cells. *Nano Letter*, B (12):4391–4397, 2008.
- [7] J.-M. Lamarre, Z. Yu, C. Harkati, S. Roorda, and L. Martinu. Optical and microstructural properties of nanocomposite Au/SiO₂ films containing particles deformed by heavy ion irradiation. *Thin Solid Films*, 479(1-2):232–237, 2005.
- [8] Nicolò Maccaferri, Juan B. González-Díaz, Stefano Bonetti, Andreas Berger, Mikko Kataja, Sebastiaan van Dijken, Josep Nogués, Valentina Bonanni, Zhaleh Pirzadeh, Alexandre Dmitriev, Johan Åkerman, and Paolo Vavassori. Polarizability and magnetoplasmonic properties of magnetic general nanoellipsoids. *Optics Express*, 21(8):9875, 2013.

- [9] Dentcho Andrey K. Sarchev and Vladimir. metal-dielectric composite filters with controlled spectral windows of transparency. *Nonlinear Optical Physics & Materials*, 12(No. 4):1–22, 2003.
- [10] D.R. Huffman C.F. Bohren. *absorption and scattering of light by small particles*. 1983.
- [11] A.V. Goncharenko. optical properties of core-shell particle composites. *chemical physics letter*, 386:25–31, 2004.
- [12] Henglein. . *phys. chem.*, 97(21):5457–5471, 1993.
- [13] Ozbay. . *Science*, 331(189), 2006.
- [14] Tobias Ambjornsson, Gautam Mukhopadhyay, S. Peter Apell, and Mikael Kall. Resonant coupling between localized plasmons and anisotropic molecular coatings in ellipsoidal metal nanoparticles. 2006.
- [15] Dylan Lu, Jimmy Kan, Eric E. Fullerton, and Zhaowei Liu. Tunable surface plasmon polaritons in Ag composite films by adding dielectrics or semiconductors. *Applied Physics Letters*, 98(24):243114, 2011.
- [16] C. Radloff N.J. Halas Prodan and P. Nordlander E. . *Science* 302, 419, 2003.
- [17] Publications Office of the European Union. Nanostructured Metamaterials. *annual series of the Official journal of the European Union*, 2010.
- [18] Andrei Stalmashonak, Gerhard Seifert, and Amin Abdolvand. Ultra-Short Pulsed Laser Engineered Metal-Glass Nanocomposites. pages 5–16, 2013.
- [19] Ji Ping Huang. Effective nonlinear optical properties of graded metal dielectric composite films of anisotropic particles. 22(8):1640–1647, 2005.
- [20] Bremen Martin-luther universit. Mie Theory 1908 2008 Mie Theory 1908 2008. 2008.
- [21] J.D. Jackson. *Classical Electrodynamics*. 1999.

- [22] Greiner W. *Classical Electrodynamics*. 1998.
- [23] Robert W. Boyd. Nonlinear Optics. *Book*, page 613, 2008.
- [24] Doyle W.T. . *Applied Physics*, 85(32323), 1999.
- [25] Whites K.W. . *Applied Physics*, 88(1962), 2000.
- [26] L.G. L.G. Grechko, V.N. Pustovit K.W. Whites. . *Physics lett.*, 76(1854), 2000.
- [27] M Y Koledintseva, R E Dubroff, and R W Schwartz. Mixtures Containing Conducting Particles At Optical Frequencies. *Progress In Electromagnetics Research Pier*, 63(1):223–242, 2006.
- [28] Ohad Levy and David Stroud. Maxwell Garnett theory for mixtures of anisotropic inclusions: Application to conducting polymers. *Physical Review B*, 56(13):8035–8046, 1997.
- [29] J M Pitarke and J B Pendry. Effective electronic response of a system of metallic cylinders. 1998.
- [30] V.N. Mal’nev and Sisay Shewamare. Slow and fast light in metal/dielectric composites with passive and active host matrices. *Physica B: Condensed Matter*, 426:52–57, 2013.
- [31] B. Abeles R.W. Cohen, G.D. Cody, M.D.Coutts. . *Physics Review*, B8(3689), 1973.
- [32] R. Gans. . *Ann. Phys.*, 37(881), 1912.

DECLARATION

I hereby declare that this thesis is my original work and has not been presented for a degree in any other University. All sources of material used for the thesis have been duly acknowledged.

Hailu Tegegn email: hailutegegndesta@gmail.com

This thesis has been submitted for examination with my approval as University advisor.

Dr.Sisay Shewamare

Jimma University email: Sisayshewa20@yahoo.com